Long-range antiferromagnetic ordering in Bi_2CuO_4

E. W. Ong
Los Alamos National Laboratory, Los Alamos, New Mexico 87545
and Department of Chemistry, Arizona State University, Tempe, Arizona 85287

G. H. Kwei and R. A. Robinson
Los Alamos National Laboratory, Los Alamos, New Mexico 87545

B. L. Ramakrishna
Department of Chemistry, Arizona State University, Tempe, Arizona 85287

R. B. Von Dreele
Los Alamos National Laboratory, Los Alamos, New Mexico 87545
(Received 1 March 1990; revised manuscript received 14 May 1990)

The results of an investigation of Bi_2CuO_4 using x-ray and neutron powder diffraction, dc magnetometry, and electron-spin resonance are presented. Simultaneous refinement of the room-temperature x-ray and neutron-diffraction data was used to obtain accurate cell parameters and atomic positions. Neutron-diffraction data at 13 and 300 K show that the appropriate space group is $P4/ncc$ at both temperatures and reveal the appearance at the lower temperature of two magnetic peaks, which can be indexed as (100) and (210) reflections. While they are clearly indicative of long-range antiferromagnetic order, on the basis of these powder data alone one cannot determine the moment direction. However, on the assumption that the moments lie along the c axis, the copper magnetic moment is $(0.56\pm0.04)\mu_B$. dc magnetometry was performed at temperatures from 1.66 to 400 K and fields ranging from 0.5 to 50 kOe. The magnetization showed no field saturation even at 1.66 K and 45 kOe. The susceptibility showed a maximum near 50.4 K with a Curie tail observed at low temperatures. Antiferromagnetic interactions dominated at all temperatures. The magnetic behavior is like that of a three-dimensional antiferromagnetic system. ESR experiments were done over the temperature range 4.3–300 K. For temperatures above 50 K, one broad line with $g=2.09$ was observed. The resonance field shifted to higher values for $T<37$ K, with an eventual splitting of the line below 15 K. These ESR signals can be associated with antiferromagnetic resonance modes, consistent with an ordered antiferromagnetic phase.

I. INTRODUCTION

The discovery of the high-transition-temperature superconductors[1] has led to a great deal of work on the structure and magnetic properties of the oxocuprates.[2,3] A number of the early studies used neutron diffraction to study antiferromagnetic ordering in La_2CuO_4 and oxygen-deficient nonsuperconducting $YBa_2Cu_3O_{6+\delta}$.[4] More recently, magnetic susceptibility, electron paramagnetic resonance and neutron-diffraction studies of related oxocuprates have been reported. Evidence for antiferromagnetic ordering has been seen in neutron powder diffraction studies of Y_2BaCuO_5 and $Y_2Cu_2O_5$.[5–7] Currently, the class of oxocuprates with the formula M_2CuO_4 (with M=rare earth), is being studied intensively. For the rare-earth cuprates, it was found that the structures adopted depended strongly on the size of the rare-earth ion, as demonstrated by the so-called T, T', and T^* phase structures. These consist of three distinct but structurally related phases whose formation is determined by the size of the rare-earth ions.[8–10] The large rare-earth ion La^{+3}, forms the T-phase structure with corner-sharing CuO_6 octahedra. The smaller rare-earth ions tend to form the T' phase with corner-sharing CuO_4 square planes. The T^* phase, which contains half a unit cell each of the T and T' phase structures, is formed when a mixture of large and small rare-earth ions occupy the now distinct M and M' sites. These contain corner-sharing CuO_5 square-planar pyramids.

One of the most interesting oxocuprates that has been studied is Bi_2CuO_4. The replacement of bismuth for the rare earths results in a radically different structure. Since the ionic radius of Bi^{+3} (1.31 Å for eightfold coordination) is nearly identical to that for La^{+3} (1.30 Å for eightfold coordination),[11] one might have expected Bi_2CuO_4 to conform to the T-phase structure. However, the difference between structures involving bismuth and lanthanum lies in the nature of the Bi—O and La—O bonds. Bismuth forms strong covalent bonds with oxygen, reducing its coordination to six, while the strongly ionic character of La—O bonds allows La^{+3} to be ninefold coordinated. Unlike many of the oxocuprates which have bridging Cu-O-Cu or Cu-O-O-Cu units made up of edge-sharing CuO_n units arranged in planar arrays, the copper ions in Bi_2CuO_4 are coordinated by square planes of oxygen ions, which are in turn stacked above each oth-

 ©1990 The American Physical Society

er in a staggered fashion, forming one-dimensional copper-ion chains. The copper atoms are not bridged by any intervening oxygen ions and the Cu-Cu distance is 2.9 Å, only slightly larger than that in metallic copper. This situation allows several possibilities for the exchange interactions between the copper ions. These may include exchange through orbital overlap as well as the superexchange through the oxygen and/or bismuth ions. The dependence of the magnetic susceptibility on temperature shows a broad maximum, typical of low-dimensional antiferromagnets, near 50 K.[3] However, the origin of its magnetic behavior is clouded somewhat by the differences in the proposed structures for Bi_2CuO_4.[12,13] The structural uncertainties and the possibility of antiferromagnetic ordering led us to undertake a joint x-ray and neutron powder diffraction study of Bi_2CuO_4 to determine its crystal and magnetic structure, at both ambient and low temperatures. Dc magnetometry was used to track its magnetic response as a function of field and temperature. Electron-spin resonance (ESR) was used to probe the local electronic environments of the copper ions. This combination of techniques provides both long- and short-range descriptions of the magnetic structure of Bi_2CuO_4.

II. RESULTS AND DISCUSSION

A. Synthesis

The Bi_2CuO_4 sample was prepared by standard powder synthesis techniques. Stoichiometric amounts of Bi_2O_3 and CuO were mixed, ground and pelletized, before baking. The pellets were baked at 780 °C for approximately 50 hrs with several regrindings in between. The samples were a metallic charcoal in appearance, but were a very dark brown after grinding.

B. Diffraction studies

X-ray diffraction patterns were taken on a Siemens D500 θ-θ diffractometer, with Cu $K\alpha$ radiation and graphite monochromator, in a single 2θ scan from 10° to 150° in 0.02° steps counting for 8 sec per step. Neutron powder diffraction data were taken on the High Intensity Powder Diffractometer (HIPD)[14] at the Manuel Lujan, Jr. Neutron Scattering Center (LANSCE). For the latter, approximately 20 g of Bi_2CuO_4, together with some He exchange gas, filled a 3/8 in. dia. thin-walled vanadium sample tube. The sample tube was mounted on a Displex He refrigerator and its temperature was controlled with a Lakeshore Cryogenics temperature controller. The data were collected in six detector banks (±153°, ±90°, and ±40°) at two sample temperatures (13 and 304 K) for approximately 8 and 6 hrs, respectively, at an average proton current of 58 μA.

The x-ray diffraction patterns indexed to the space group $P4/ncc$ given by Boivin *et al.*[12] rather than the $I4$ space group reported by Arpe and Müller-Buschbaum.[13] The latter space group failed to account for at least three prominent diffraction peaks in the pattern. Subsequently, we refined both the room- and low-temperature structures in the $P4/ncc$ space group using the Rietveld refinement codes, Generalized Structure Analysis System (GSAS) developed by Larson and Von Dreele.[15] For the room-temperature data, we combined x-ray and neutron data in the structural refinement[16] in order to constrain the refinement more tightly and to refine the neutron powder diffractometer constants to the lattice constants determined from the well-known Cu $K\alpha$ wavelength.[17] For the structure at 13 K, we did not refine the neutron diffractometer constants, but instead used the refined values from the room-temperature refinement. Otherwise, both refinements were done in the same way. We began the structural refinements with the structure given by Boivin *et al.*[18] and then refined lattice constants, atomic positions, anisotropic thermal parameters, profile coefficients (which included anisotropic strain), absorption and preferred orientation. Portions of both the x-ray and neutron data for Bi_2CuO_4 at 304 K, together with the fit from the refined structure are shown in Fig. 1. The resulting structural parameters are given in Table I. The structure at both temperatures is similar to that reported to Boivin *et al.*[18] This structure is illustrated in the Oak Ridge Thermal Ellipsoid Plot Program ORTEP (Ref. 19) plots shown in Figs. 2 and 3. The bond lengths of selected bonds are shown in Table II.

Below the peak in magnetic susceptibility, at 13 K, two extra reflections were observed as can be seen in Fig. 4. These can be indexed as (100) and (210), respectively, in the tetragonal cell. These reflections are indicative of

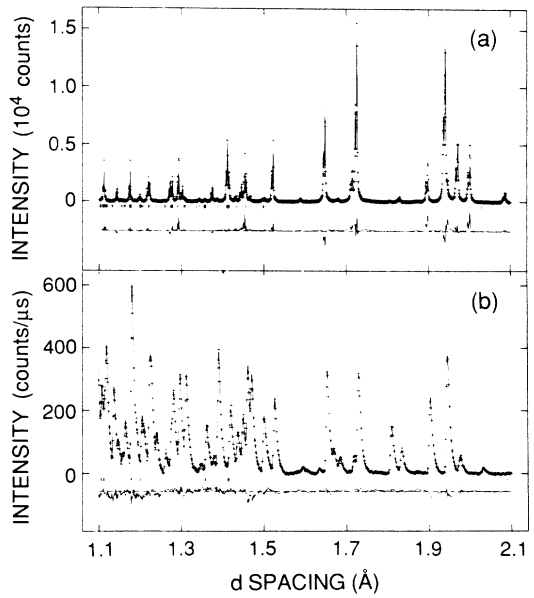

FIG. 1. Part of the x-ray and neutron-diffraction data for Bi_2CuO_4 at 304 K. Data shown by plus (+) marks in (a) represent only data collected on the +153° detector bank of HIPD while data shown in (b) were taken on a Siemens D500 x-ray diffractometer. The continuous line through both sets of data is the calculated profile from Rietveld refinement. Tick marks below the data indicate the positions for the allowed reflections. Both Cu $K\alpha_1$ and $K\alpha_2$ positions are marked in the x-ray pattern; the d spacings are computed from $K\alpha_1$. The lower curve in each panel represents the difference between the observed and calculated profiles.

TABLE I. Refined structural parameters for Bi_2CuO_4 at 13 and 304 K. Space group $P4/ncc$. Atomic positions: Bi($x, x-\frac{1}{2}, \frac{1}{4}$) Cu ($\frac{3}{4}, \frac{3}{4}, z$), and O($x, y, z$).

		13 K	304 K
a(Å)		8.4993(5)	8.5002(1)
c(Å)		5.7962(3)	5.8176(1)
V(Å^3)		418.71(7)	420.34(1)
Bi	f	1	1
	x	0.918 41(3)	0.918 70(4)
	$U_{11}=U_{22}$	0.19(1)	0.70(2)
	U_{33}	0.20(2)	0.73(3)
Cu	f	1	1
	z	0.077 65(13)	0.077 99(17)
	$U_{11}=U_{22}$	0.24(2)	0.53(3)
	U_{33}	0.50(3)	1.02(5)
O	f	1.005(1)	1.006(2)
	x	0.049 66(5)	0.049 27(6)
	y	0.358 06(4)	0.357 96(6)
	z	−0.091 54(9)	−0.091 52(13)
	U_{11}	0.46(2)	0.89(3)
	U_{22}	0.31(2)	0.58(3)
	U_{33}	0.46(2)	1.20(4)
Rwp/Rexp		3.15/2.28	4.75/2.96

[a]Thermal parameters are in units of 100 Å^2. Agreement factors are in percent. The numbers in parentheses following refined parameters represent one estimated standard deviation in the last significant digit(s).

long-range antiferromagnetic order, in which the copper atoms at $[\frac{1}{4}\frac{1}{4}z]$ and $[\frac{1}{4}\frac{1}{4}z+\frac{1}{2}]$ are polarized antiparallel to the copper atoms at $[\frac{3}{4}\frac{3}{4}-z]$ and $[\frac{3}{4}\frac{3}{4}\frac{1}{2}-z]$ as shown in Fig. 5. It is well known that, with powder data alone, one can only determine the angle ϕ between the fourfold axis and the moment direction.[20] In fact, with only $l=0$ reflections like the (100) and (210) that we observe, it is not even possible to determine that angle. Neglecting the

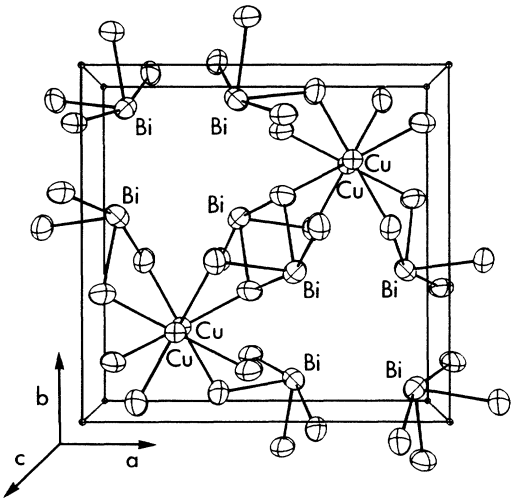

FIG. 2. The view of the structure of Bi_2CuO_4 showing the staggered CuO_4 square-planar units and their coordination to the Bi chains along the c axis. The box designates the unit cell; all Bi and Cu ions are labeled, and unlabeled atoms are O ions. Thermal ellipsoids are drawn as 97% probability surfaces.

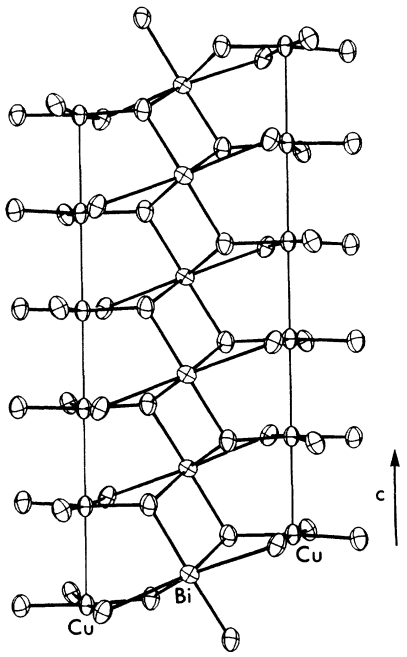

FIG. 3. The vertical stacking of the CuO_4 planes for three unit cells along the c axis viewed perpendicular to the c axis; here again, Bi and Cu are labeled only in the first layer, where the O ions are again unlabeled. Lines connecting the Cu ions have been drawn to accentuate the linear Cu chains. Thermal ellipsoids are drawn as 97% probability surfaces.

form factor and the Debye-Waller factor, the intensities of the (100), (210), (300), and (002) (the longest d-spacing reflection with $l\neq 0$) reflections are given by

$$I_{100}=I_{300}=16(2-\sin^2\phi)\ , \tag{1}$$

$$I_{210}=16(4-2\sin^2\phi)=2I_{100}\ , \tag{2}$$

and

$$I_{002}=16\sin^2\phi\sin^2(4\pi z)\ . \tag{3}$$

The observed relative intensities of the (100) and (210) reflections, after correction for the Lorentz factor and magnetic form factor[21] are in reasonable agreement with these expressions. A similar analysis for the (300)

TABLE II. Bond distances for the constituents of Bi_2CuO_4 at 13 and 304 K.

		13 K	304 K
Cu—O	(4x)	1.9364(4)	1.9390(5)
Cu—Bi	(2x)	3.3151(3)	3.3148(3)
Bi—O	(2x)	2.1276(5)	2.1280(6)
	(2x)	2.7585(4)	2.7590(6)
	(2x)	2.3294(5)	2.3336(7)
Cu—Cu	(2x)	2.898 07(17)	2.908 82(2)
Bi—Bi	(2x)	3.4995(4)	3.5045(5)

[a]The numbers in parentheses following the derived bond distances represent one estimated standard deviation in the last significant digit.

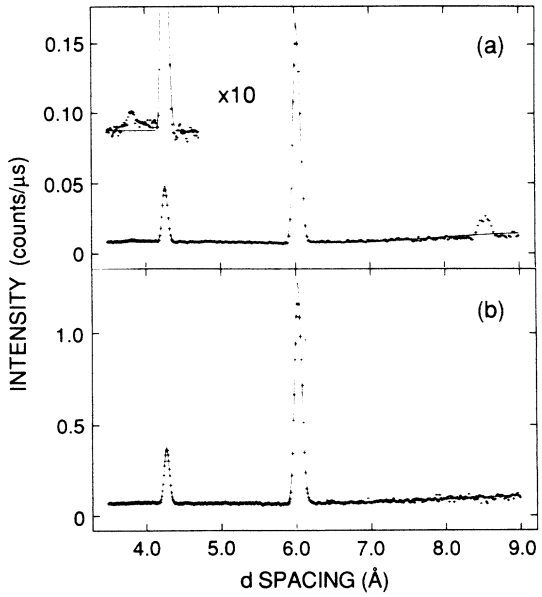

FIG. 4. Comparison of portions of the neutron powder diffraction patterns measured on the $-40°$ detector bank for Bi_2CuO_4 at 13 and 304 K. Panel (a) shows the normalized data in the d spacing range 3.5–9.0 Å taken at 13 K with the magnetic peaks at d spacings of 3.8 and 8.5 Å, while panel (b) shows the data taken at 304 K.

reflection shows that it is below the sensitivity of our measurement. As for the (002) reflection, even in the most favorable case when $\phi=90°$ (which corresponds to in-plane moments), its intensity is almost an order of magnitude lower than that of the (210) reflection, which is only just visible in our data. Given that it occurs at a shorter d spacing and is coincident with a nuclear peak, there is no prospect of extracting a value of ϕ from our data. Furthermore, the moment that one might extract from our diffraction patterns is dependent on ϕ: from Eqs. (1) and (2)

$$\mu^2 \propto 2-\sin^2\phi \ . \tag{4}$$

During the course of this work, a similar study of Bi_2CuO_4 was published by Attfield.[22] His experiment was performed on a new state-of-the-art reactor powder diffractometer designed to take rapid sequential diffraction patterns, whereas ours was performed on a relatively simple high-intensity low-resolution powder diffractometer at a pulsed spallation source. The conventional wisdom is that such magnetic experiments are better done at reactor sources. Nevertheless, Attfield was only able to observe the same two reflections. He analyzed his data assuming that the moments are parallel to the c-axis (i.e., that $\phi=0$). If we make the same assumption, we obtain a moment of $(0.56\pm0.04)\mu_B$ which is consistent with his result. As far as we are aware, this is the first time that magnetic ordering on the copper sublattice has been observed in such an oxocuprate system by means of neutron powder diffraction at a spallation source. All one needs is a set of detectors at low scattering angles (40° in our case) so that the large d spacing magnetic reflections become accessible.

C. Dc magnetization studies

The SQUID magnetometer used in this study has been described elsewhere.[5] The temperature and magnetic-field range probed are 1.66 to 400 K and 0.5 to 45 kOe, respectively. The magnetization of Bi_2CuO_4 responded linearly with applied field strength, showing no field saturation even at 1.66 K and 45 kOe. The molar susceptibility χ increased upon cooling from 400 K, reaching a broad maximum near 50 K ($T_{\chi_{max}}$) and then decreases upon further cooling. Below 20 K, a Curie-like tail is evident, similar to earlier observations.[23] A plot of χT versus T is shown in Fig. 6. Note that χT (proportional to the square of the average moment) does not level off even at high temperatures. This indicates that the magnetic behavior of the copper ions in Bi_2CuO_4 near room temperature is not strictly that of a set of isolated paramagnetic ions. The effective magnetic moment per

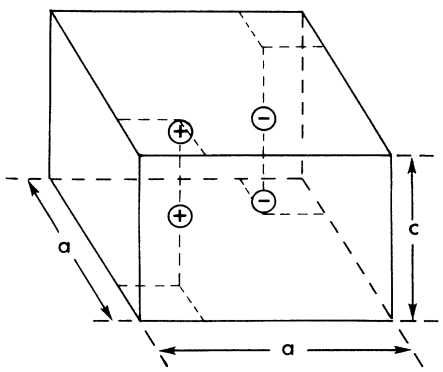

FIG. 5. The antiferromagnetic spin structure for Bi_2CuO_4. Only the copper atoms are shown for simplicity.

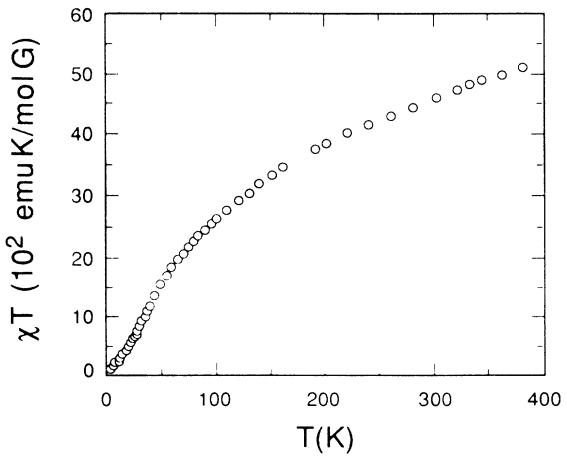

FIG. 6. The variation of χT (proportional to μ_{eff}^2) with temperature. The decrease as $T\rightarrow 0$ is indicative of antiferromagnetic interactions. Note that even at 400 K, it does not flatten out, consistent with strong exchange between the copper ions.

copper ion in Bi_2CuO_4 was found to be $(0.47\pm0.06)\mu_B$ and $(1.50\pm0.08)\mu_B$ at 13 and 300 K, respectively. The low-temperature result is comparable with the ordered moment found from neutron scattering (see preceding section). The room-temperature moment is very close to those found for Cu(II) carboxylates, typically 1.4 μ_B per ion. The magnetic moments of simple Cu(II) compounds generally lie in the range $(1.73-2.20)\mu_B$. Figure 7 shows a plot of $1/\chi$ versus T, indicating that antiferromagnetic interactions are dominant at high as well as low temperatures. Fitting the high-temperature data to the formula $\chi=C/(T+\Theta)$ yields a large Weiss constant Θ of 229 K. These combined results indicate that antiferromagnetic interactions are dominant in this compound, with any ferromagnetic interaction rather feeble. Attfield[22] determined the Néel point T_N to be 41.9±0.5 K. This is consistent with our neutron results showing ordering well below that. The ratio of $T_N/T_{\chi_{max}}=0.83$ which is obtained by combining Attfield's result and our susceptibility data, implies that Bi_2CuO_4 behaves nearly like a three-dimensional Heisenberg antiferromagnet. This is in accordance with an established empirical criterion for determining the spatial dimensionality of a magnetic system. It gives $T_N/T_{\chi_{max}}$: (1) >0.9 for three dimensional, (2) 0.25 to 0.5 for two dimensional, and (3) <0.1 for good one-dimensional systems.[24,25] The fact that our ratio is slightly lower than expected indicates a slight tendency toward short-range ordering. To date, no high-temperature series expansions are available for simulating the magnetic behavior of three-dimensional Heisenberg systems. An estimate for the effective antiferromagnetic exchange parameter can be made, within the mean-field approximation, from the relationship:[24]

$$\chi_\perp(0)=Ng_\perp^2\mu_B^2/4z|J_{AF}^{eff}| \ . \tag{5}$$

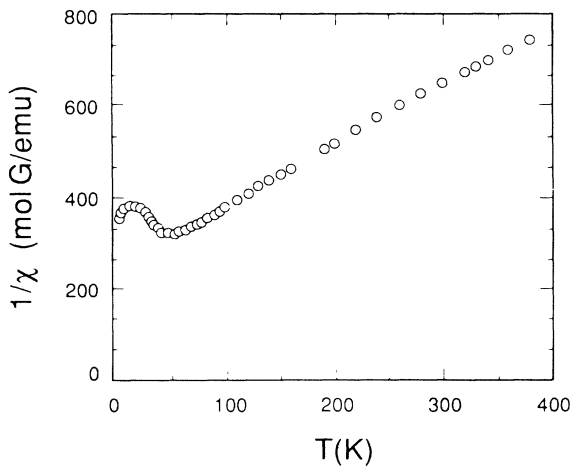

FIG. 7. The variation of inverse magnetic susceptibility with temperature at $H=0.5$ kOe. The minimum near 50.4 K is very close to the Néel point at 41.9 K. This feature shifts slightly to higher temperatures with increasing field strength. The fact that the high-temperature data extrapolates back to negative temperatures indicates that antiferromagnetic interactions are dominant at all temperatures.

Taking the susceptibility maximum $(3.11\times10^{-3}$ emu/mol Oe) of our powder data as an approximation to the susceptibility perpendicular to the easy axis of the antiferromagnet at 0 K, and taking $g_\perp=2.09$ from ESR data (where N is Avogadro's number, μ_B is a Bohr magneton, and z is the number of nearest Cu neighbors), we get

$$2z|J_{AF}|/k_B=264 \text{ K} \tag{6}$$

indicating an exchange integral typical of strong antiferromagnets.[24,26] A comparison with earlier models will be made in the following.

Attfield[22] proposed a model in which the copper ions in the compound were coupled with ferromagnetic intrachain and antiferromagnetic interchain exchanges. The ferromagnetic and antiferromagnetic exchange parameters derived from his neutron results were reported as +190 and −90 K, respectively. These parameters imply that the competing antiferromagnetic and ferromagnetic interactions are comparable in size and this is inconsistent with our data, which indicate that the dominant interactions are antiferromagnetic. Sreedhar and Ganguly[3] proposed a spin-Peierls transition as a possible mechanism responsible for the observed temperature dependence of the magnetic susceptibility, before it was known that Bi_2CuO_4 ordered as found here and by Attfield.[22] Our neutron data, discussed above, showed no indications of dimerization for the copper ions down to 13 K. The broad maximum in the susceptibility response to temperature was not found to be very field sensitive, with $T\chi_{max}=50.4$ at 0.5 kOe and changing to 52 K at 45 kOe, is a slight field enhancement. This behavior is consistent with three-dimensional ordering, where the ordering temperature is enhanced initially with increasing magnetic field.[27] The "ordering" temperature would be suppressed with increasing magnetic-field strength in spin-Peierls cases.[28]

Based on the crystal structure and assuming ionic bonds between the atoms, one would expect a one-dimensional chainlike magnetic behavior for Bi_2CuO_4. The intrachain exchange interactions would be stronger than those between chains, giving the compound a moderate degree of magnetic anisotropy. However, it was found to behave more like a three-dimensional system. This indicates that the intrachain and interchain interactions are of comparable magnitude. From crystal-field theory, the unpaired electron in Cu^{+2} should reside in a $d_{x^2-y^2}$ orbital, as a result of the square-planar coordination of copper by the oxygen ions. An eclipsed conformation of the CuO_4 squares along the c axis favors antiparallel alignment of the electrons, leading to antiferromagnetic interactions as observed in copper acetate.[29] Our x-ray and neutron-diffraction results conformed with the $P4/ncc$ space group, implying that the CuO_4 planes are staggered along the c axis. Hence in accordance with Hund's rule, because of the orthogonality of the orbitals, direct Cu-Cu coupling will be ferromagnetic. On the contrary, it was found that the dominant interactions are antiferromagnetic. The somewhat unexpected results of three-dimensional exchange and the dominance of anti-

ferromagnetic interactions can be explained by covalent bonding in the structure. The energies of bismuth, oxygen, and copper orbitals (Bi 6*s*, O 2*p*, and Cu 3*d*) are of comparable magnitude. Thus, the Bi—O and Cu—O bonds formed by the overlap of the oxygen lone pairs with the metal orbitals are strongly covalent. These covalent bonds can form a three-dimensional network of superexchange pathways.[30] The unpaired electrons in the copper orbitals, can be expected to be strongly correlated antiferromagnetically in the *x-y* plane as well as along the *c* axis through Cu-O-Bi-O-Cu networks.

D. Electron spin resonance studies

ESR and antiferromagnetic resonance measurements were made at *X*-band frequencies for temperatures ranging from 4.3 to 300 K, and at *Q*-band frequencies at 300 K. The spectrometer and its cryogenic accessories have also been described previously.[5] From 300 K down to 50 K, we observed a single broad signal (ca 2200 G wide) with a constant *g* value close to 2.09. This is similar to that reported by Sreedhar and Ganguly.[3] However, the resonant field for the signal shifted toward higher values upon further cooling. The evolution of the signal is shown in Fig. 8 at selected temperatures. The resonant field variation with temperature is plotted in Fig. 9. The

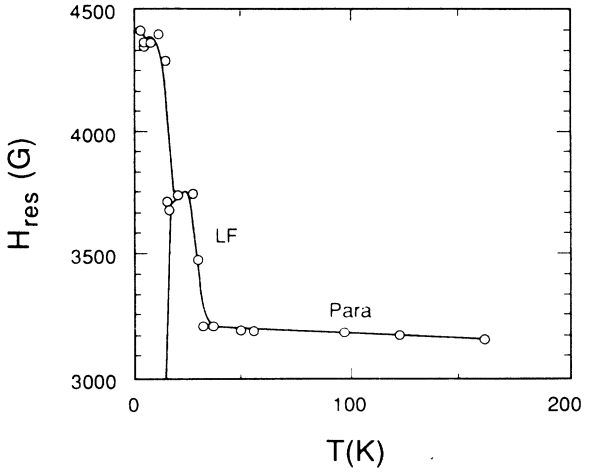

FIG. 9. Evolution of the resonance signals with temperature (solid lines only provide guides to the eye). Above 50 K, the signal is an exchange averaged paramagnetic signal. Below the Néel point, the signal shifts to higher frequencies, tentatively assigned as the "low frequency" antiferromagnetic resonance mode. The apparent splitting of the signal below 15 K is not understood. The position of the lower resonance field is omitted in the plot due to its large uncertainty resulting from overlapping of the lines.

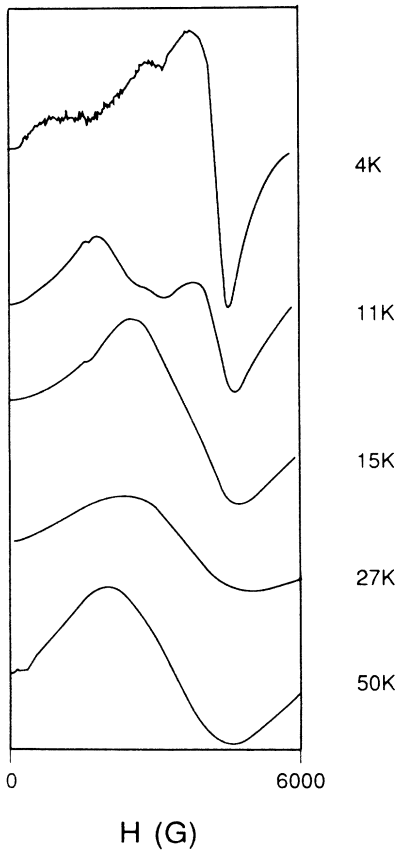

FIG. 8. Change of line shape for the resonance signals with temperature. Note the complicated behavior below 15 K. Two overlapped signals are evident at low temperatures.

shifting of the resonant fields below 40 K could be explained either by local fields due to three-dimensional ordering or the effect of correlation from short-ranged ordering.[31] We favor the idea that three-dimensional ordering is responsible, as this also gives rise to antiferromagnetic resonance. In general, antiferromagnetic resonance modes for antiferromagnets possessing strong exchange interactions and large magnetic anisotropy cannot be observed using *X*-band frequencies. For a uniaxial antiferromagnet, the resonance fields for directions parallel and perpendicular to the "easy" axis are given by[32]

$$H_{\rm res}=[(\omega/\gamma)^2+2H_E H_A]^{1/2} \tag{7}$$

and

$$H_{\rm res}=[(\omega/\gamma)^2-2H_E H_A]^{1/2}\,, \tag{8}$$

respectively, where H_E and H_A are the exchange and anisotropy fields. The resonance field for the paramagnetic signal is given by ω/γ. In any direction, antiferromagnetic resonance can be observed only if the product of the exchange field and the anisotropy field is not very large. The fact that the Néel temperature is relatively high indicates that H_E is large (ca 10^5 G). The fact that we can observe antiferromagnetic resonance thus implies that H_A must be very small (ca. a few Gauss). This small anisotropy is consistent with the compound's three-dimensional bulk magnetic behavior, discussed above. A similar combination of strong exchange with weak anisotropy has been found in $RbMnF_3$.[32] The small exchange anisotropy in $RbMnF_3$ results from the half-filled *d* shell in Mn^{+2}, which has an orbital *S* ground state. Cu(II) on the other hand, having a *D* orbital ground state, should

be anisotropic. In Bi_2CuO_4 the strong crystal fields around Cu^{+2}, resulting from its coordination by the oxygen ions, may have quenched the orbital angular momentum of its electrons leading to small single ion anisotropy. From the temperature behavior of the signal, in comparison with antiferromagnetic resonance studies reported for systems well studied by others,[32-35] we have arrived at the following tentative assignments. The high-temperature signal ($T > 50$ K), with constant g value of 2.09 ($H_{res} = 3200$ G, is the exchange averaged paramagnetic signal of the copper ions above the Néel point. This signal should evolve into the high-frequency mode in a narrow temperature range just above the Néel point, which shows a shift to lower resonant fields.[33] Unfortunately, because of the roughness of our temperature increments due to slight temperature fluctuations, we did not observe this mode. Below the Néel point, the signal should evolve into the low-frequency mode.[33] The shift to higher fields on cooling, with eventual onset of a plateau, is consistent with the behavior of the low frequency mode. The observation of two signals for temperatures below 15 K (an apparent split) cannot be explained at this time. Variable power experiments were performed at 5 K in an attempt to determine the origin of the two signals. With increasing power (up to 200 mW), the high field signal was not saturated. The low field signal seems to exhibit interference effects, which are not yet understood but may be similar to those observed earlier in another system.[36] No other signals were observed with fields up to 17 kOe at X-band frequencies. Because of the presence of strong antiferromagnetic interactions in this system, higher frequencies may be needed to observe the other modes. Further studies on the antiferromagnetic resonance mode will be performed by measuring the orientational and temperature dependence of the resonant fields in a single crystal, if and when one becomes available.

III. SUMMARY

In summary, we have confirmed that the space group for Bi_2CuO_4 is $P4/ncc$ rather than $I4$. We have refined the structural parameters using both x-ray and neutron data at room temperature, and using neutron data at 13 K. Our positional parameters are in agreement with those of Attfield,[22] with comparable or slightly higher precision. The more highly constrained nature of the simultaneous x-ray and neutron refinement of room-temperature data is likely to give better values for all structural parameters, such as lattice constants and both positions and thermal parameters. We see two extra peaks at low temperature in the neutron data that are indicative of long-range antiferromagnetic order. This is consistent with our susceptibility data which give a peak at about 50 K and a Weiss constant of 229 K, indicating that antiferromagnetic interactions dominate at all temperatures. Our ESR measurements probe the local magnetic environment of the Cu ions. While the high-temperature behavior is characteristic of paramagnetism, with antiferromagnetic interactions, below 50 K there are antiferromagnetic resonance modes. Both observations are consistent with the onset of long-range antiferromagnetic order at about 50 K, and Bi_2CuO_4 behaves like a three-dimensional antiferromagnet with long-range magnetic order below this temperature. The behavior below 15 K is not well understood, but can probably be resolved if and when single crystals of Bi_2CuO_4 become available.

ACKNOWLEDGMENTS

We thank A. C. Lawson, J. A. Goldstone, R. D. Willett, and J. B. Goodenough for a number of useful discussions. We are indebted to the late A. Williams who built the powder diffractometer with the well-shielded low-angle detector banks that were crucial to these magnetic neutron-scattering experiments. We also acknowledge the use of the Magnetism and Magnetic Resonance Facility at Arizona State University. This work was supported in part by the Division of Materials Sciences, Office of Basic Energy Sciences of the U.S. Department of Energy.

[1] J. G. Bednorz and K. A. Müller, Z. Phys. B **64**, 189 (1986).
[2] B. L. Ramakrishna and E. W. Ong, J. Appl. Phys. **64**, 5953 (1988).
[3] K. Sreedhar and P. Ganguly, Inorg. Chem. **27**, 2261 (1988).
[4] See S. K. Sinha, D. Vaknin, M. S. Alvarez, A. J. Jacobson, J. Newsam, J. T. Lewandowski, D. C. Johnston, C. Stassis, J. M. Tranquada, T. Freltoft, H. Moudden, A. I. Goldman, P. Zolliker, D. E. Cox, and G. Shirane, Physica B **156**, & **157**, 854 (1989), and references therein.
[5] E. W. Ong, B. L. Ramakrishna, and Z. Iqbal, Solid State. Commun. **66**, 171 (1988).
[6] T. Chattopadhyay, P. J. Brown, U. Köbler, and M. Wilhelm, Europhys. Lett. **8**, 685 (1989).
[7] J. Aride, S. Flandrois, M. Taibi, A. Boukhari, M. Drillan, and J. L. Soubeyroux, Solid State Commun. **72**, 459 (1989).
[8] S-W. Cheong, Z. Fisk, J. D. Thompson, and R. B. Schwartz, Physica C **159**, 407 (1989).
[9] J. Akimitsu, S. Suzuki, M. Watanabe, and H. Sawa, Jpn. J. Appl. Phys. **27**, L1859 (1989).
[10] Y. Tokura, H. Takagi, and S. Ushida, Nature **337**, 345 (1989).
[11] R. D. Shannon and C. T. Prewitt, Acta Crystallogr. Sec. B **25**, 925 (1969).
[12] J.-C. Boivin, D. Thomas, and G. Tridot, C. R. Acad. Sci. Paris **276**, 1105 (1973).
[13] R. Arpe and Hk. Müller-Buschbaum, Z. Anorg. Chem. **426**, 1 (1976).
[14] Los Alamos National Laboratory Report No. LA-LP-88-4, 1988 (unpublished).
[15] A. C. Larson and R. B. Von Dreele, Los Alamos National Laboratory Report No. LA-UR-86-748, 1987 (unpublished).
[16] A. Williams, G. H. Kwei, R. B. Von Dreele, A. C. Larson, I. D. Raistrick, and D. L. Bish, Phys. Rev. B **37**, 7960 (1988).
[17] R. D. Deslattes and A. Henins, Phys. Rev. Lett. **31**, 972 (1973).

[18]J.-C. Boivin, J. Trehoux, and D. Thomas, Bull. Soc. Miner. Crystallogr. **99**, 193 (1976).
[19]C. K. Johnson, Oak Ridge National Laboratory Report ORNL-5138, 1976 (unpublished).
[20]G. Shirane, Acta Crystallogr. **12**, 282 (1959).
[21]A. J. Freeman and R. E. Watson, Acta Crystallogr. **14**, 231 (1961).
[22]J. P. Attfield, J. Phys., Condens. Matter **1**, 7045 (1989).
[23]K. Sreedhar, P. Ganguly, and S. Ramasesha, J. Phys. C **21**, 1129 (1988).
[24]L. J. de Jongh and A. R. Miedema, Adv. Phys. **23**, 1 (1974).
[25]I. S. Jacobs, J. W. Bray, H. R. Hart, Jr., L. V. Interrante, J. S. Kasper, G. D. Watkins, D. E. Prober, and J. C. Bonner, Phys. Rev. B **14**, 3036 (1976).
[26]P. W. Selwood, *Magnetochemistry* (Interscience, New York, 1964), p. 328.
[27]W. J. M. de Jonge, J. P. A. M. Hijmans, F. Boersma, J. C. Schouten, and K. Kopinga, Phys. Rev. B **17**, 2922 (1978).
[28]J. A. Northby, H. A. Groenendijk, L. J. de Jongh, J. C. Bonner, I. S. Jacobs, and L. V. Interrante, Phys. Rev. B **25**, 3215 (1982).
[29]R. L. Carlin and A. J. Van Duyneveldt, *Magnetic Properties of Transition Metal Compounds* (Springer, New York, 1977), p. 86.
[30]J. B. Goodenough (private communication).
[31]K. Nagata and Y. Tazuke, J. Phys. Soc. Jpn. **32**, 337 (1972).
[32]D. T. Teaney and M. J. Freiser, Phys. Rev. Lett. **9**, 212 (1962).
[33]N. J. Zimmerman and A. J. Van Duyneveldt, Physica **90B**, 119 (1977).
[34]J. Ubbink, J. A. Poulis, H. J. Gerritsen, and C. J. Gorter, Physica **18**, 23 (1952).
[35]R. D. Willett, D. Barberis, and F. Waldner, J. Appl. Phys. **53**, 2677 (1982).
[36]H. Reimann, H. Hagen, F. Waldner, W. Berlinger, and H. Arend, Solid State Commun. **17**, 1319 (1975).